

## Article

# Recovery of Ionic Liquid from the Model Solution Mixture Mimicking the Catalytically Hydrolyzed Cellulose Product Utilizing Amberlyst Ion-Exchange Resin

Chhabilal Regmi <sup>1,\*</sup>, Chidambaram Thamaraiselvan <sup>1,2</sup> , Zhexi Zhu <sup>3</sup>, Xianghong Qian <sup>3</sup> and S. Ranil Wickramasinghe <sup>1,\*</sup>

<sup>1</sup> Ralph E. Martin Department of Chemical Engineering, University of Arkansas, Fayetteville, AR 72701, USA

<sup>2</sup> Interdisciplinary Centre for Energy Research, Indian Institute of Science, Bangalore 560012, India

<sup>3</sup> Department of Biomedical Engineering, University of Arkansas, Fayetteville, AR 72701, USA

\* Correspondence: cregmi@uark.edu (C.R.); swickram@uark.edu (S.R.W.)

**Abstract:** The hydrolysis of cellulose using ionic liquid (IL) has been extensively studied but there is limited understanding of the removal of IL from the biomass hydrolysate. Finding a suitable method for the recovery and reuse of IL is one of the biggest challenges before its large-scale application. Selecting an appropriate combined recovery process is very important. This study proposed a facile ion-exchange combined method for the recovery of IL from the modeled cellulose hydrolysate mixture containing sugars as well as  $\gamma$ -valerolactone (GVL) via an adsorption–desorption mechanism using sulfonic acid cation-exchange (Amberlyst 15 (H)) resin. The results showed that the resin could adsorb more than 94% of 1-ethyl-3-methylimidazolium chloride [Emim]Cl IL at ambient conditions within a contact time of 20 min. The other coexisting constituents like glucose and GVL have no significant effect on the adsorption efficiency of IL. The adsorption of IL on Amberlyst 15 (H) resin was observed to be pseudo-second-order adsorption. The regeneration of the adsorbed IL was possible up to 70% using low-cost, easily available sodium chloride (NaCl) solution. Similarly, despite the interference of other unwanted byproducts in the real biomass hydrolysate sample, an IL adsorption efficiency up to 51% was reached under similar operating conditions. This study thus opens the facile possibility of extracting and recycling IL used in the biomass hydrolysis process.

**Keywords:** ionic liquid; adsorption; cation-exchange resin; Amberlyst; desorption; NaCl



**Citation:** Regmi, C.; Thamaraiselvan, C.; Zhu, Z.; Qian, X.; Wickramasinghe, S.R. Recovery of Ionic Liquid from the Model Solution Mixture Mimicking the Catalytically Hydrolyzed Cellulose Product Utilizing Amberlyst Ion-Exchange Resin. *Processes* **2024**, *12*, 55. <https://doi.org/10.3390/pr12010055>

Academic Editors: Carlos Manuel Silva, José Aniceto and Inês Portugal

Received: 30 November 2023

Revised: 15 December 2023

Accepted: 19 December 2023

Published: 26 December 2023



**Copyright:** © 2023 by the authors. Licensee MDPI, Basel, Switzerland. This article is an open access article distributed under the terms and conditions of the Creative Commons Attribution (CC BY) license (<https://creativecommons.org/licenses/by/4.0/>).

## 1. Introduction

Utilizing abundant lignocellulosic biomass for biofuel production helps minimize greenhouse gas emissions and reduce environmental impact [1]. The efficient use of lignocellulosic biomass for biofuel production requires a particular fragmentation of its components in the pre-stages. Separating cellulose from lignin with minimal polymer degradation is challenging due to the stiffness of the crosslinked matrix [2]. A pretreatment method is usually required to overcome the hurdle. Normally, the pretreatment process changes the structure of the biomass by breaking its cell wall and making the cellulose and hemicellulose easier for hydrolysis [3]. Conventional biomass pretreatment methods, like steam explosion and acid/alkali treatments, lack industrial scalability due to harsh conditions leading to byproducts, inhibited hydrolysis, and decreased sugar yields [4]. Issues like equipment corrosion, hazardous chemicals, and high energy consumption further hinder their applicability [5–7]. The scientific community faces a critical challenge in developing alternative solvents and technologies. The use of IL for biomass processing, such as pretreatment, hydrolysis, or fractionation, is considered innovative due to unique alterations in biomass physicochemical properties not seen in other solvent systems [8]. In the lignocellulosic biomass hydrolysis process, IL modifies the cell wall structure, thus reducing cellulose crystallinity, increasing cellulose surface accessibility, and promoting

biomass swelling [9]. The cations and anion in IL affect biomass solubility and water interaction, making it a promising solvent [10,11]. Although IL proved to be a very promising solvent for lignocellulose biomass conversion, the high cost of its fabrication limits its upscale application. Current research focuses on cost-effective recycling strategies to minimize the environmental impact and promote ILs' reuse [12].

ILs are non-molecular compounds with tunable properties for diverse applications [13,14]. Among others, imidazolium-based ILs, particularly with  $\text{Cl}^-$  anion, exhibit enhanced cellulose interaction [15,16]. ILs are even recognized for catalytic roles in chemical reactions, serving as green solvents due to advantages over traditional ones [17]. The low vapor pressure of ILs alleviate the air pollution because of the nominal evaporation during operation. Their liquid nature over a wide range of temperature contribute to their utilization as a solvent in a variety of fields such as organic synthesis, nanoparticles synthesis, as well as various extraction process of industrial significance [18]. The high melting point and thermal stability allow ILs to combat intensive operational conditions of temperature and pressure [19]. The non-volatility and non-flammability characteristics minimize the exposure risk and solvent loss due to evaporation [20]. Despite the drawbacks like reactivity and toxicity, ILs' desirable properties make them ideal solvents for environmentally friendly processes for biomass conversion. Thus, to minimize the production cost, maximize its large-scale application, and promote the sustainability, developing efficient ILs separation and recovery techniques are crucial [12].

Choosing an effective separation method for ILs depends on various factors such as ILs characteristics, energy requirements, product purity, equipment availability, and cost [12]. While some methods show better performance, many are limited by efficiency, resulting in impurities or high operating costs [12]. Distillation, a traditional approach, and even its improved technologies face challenges like the low distillation rate, high energy consumption, and necessity of harsh operation conditions (high vacuum and high temperature) [21,22]. Liquid-liquid extraction suffers from cross-contamination and poor phase separation that results in low efficiency [22]. Membrane-based techniques like nanofiltration, reverse osmosis, and pervaporation are energy-efficient but have limitations. Nanofiltration and reverse osmosis are simple, less energy- and solvent-demanding processes but osmotic pressure is a limiting factor. Similarly, in pervaporation, the presence of ILs decreases the water activity, thus resulting in relatively low flux and recovery yield [22–24]. Magnetic extraction, although efficient and low energy, is limited to ILs responsive to magnetic fields. Developing cost-effective and efficient IL recovery techniques remains a key focus for researchers [25].

Recovering essential organic solvents (ILs/GVL) from cellulose hydrolysate, which contains fractionation solvent, fragmented lignin, and degradation products, is crucial. Distillation is often preferred but faces challenges due to the non-volatility of GVL/ILs, leading to high energy costs [26]. Adsorption emerges as an eco-friendly, robust, and cost-effective method for recovery, surpassing extraction in terms of efficiency and purity [27,28]. Activated carbon [29] and clays [30] are the extensively researched adsorbents, while ion-exchange resins stand out for their fast kinetics, high treatment capacity, and effective low-concentration residue separation [31]. Surface modification with different ligands further enhances their binding capacities, increasing separation affinity [32].

Amberlyst, a microporous resin, stands out for its high surface area and active sites, making it ideal for ion-exchange processes. Noteworthy for its chemical stability, eco-friendliness, non-toxicity, low cost, and recyclability, it has been extensively studied for various applications [33]. For instance, Amberlyst A-12 efficiently removes sulfate, showing rapid sorption and nearly complete desorption [34]. Amberlyst A-23/A-24 resins exhibit strong sorption of Pd(II) ions, with A-23 demonstrating higher capacity [35]. Amberlyst 15, another microporous resin, is effective in adsorbing heavy metal ions, dyes, and volatile compounds. It shows significant removal percentages for ions like Cr(III), Cd(II), malachite green, and ammonium ion. Amberlyst resins, with their versatility and efficiency, are thus playing a crucial role in diverse adsorption applications [33,35–38].

Although the choice of ion-exchange resins is very well established unit operation, its use in industrial processes has consistently expanded, resulting in green techniques and processes that widen the initial and most commonly applied areas of water purification and demineralization [39]. Despite the scarcity of studies on the use of ion-exchange resins in organic medium, understanding adsorption isotherms and ion-exchange mechanisms of ILs from a biomass hydrolysate mixture, including GVL, is crucial. This exploration suggests a novel purification/separation technique for organic solutions. Notably, there are no studies of ion-exchange resins being employed for separating ILs from biomass-hydrolyzed mixtures, as per the authors' knowledge. This study aims to assess the sorption potential of the cationic exchange resin (Amberlyst A-15) for separating ILs from a mixture containing IL, GVL, and sugar—a significant component of cellulose-hydrolyzed products. The research showcases potential applications in ILs removal, separation, and recovery from biomass hydrolysis processes. The study explores influencing factors for IL adsorption from the GVL, glucose, and IL mixture, including the subsequent desorption of the IL.

## 2. Materials and Methods

### 2.1. Materials

Ionic liquid, 1-ethyl-3-methylimidazolium chloride ( $C_6H_{11}N_2Cl$ ) ( $\geq 95\%$ ), acronymized as [Emim]Cl, was purchased from Sigma-Aldrich, St. Louis, MO, USA. The ion-exchange resin (Amberlyst<sup>®</sup>15 (H)) was purchased from Thermo Scientific, Waltham, MA, USA. The information about the physical and chemical properties of the resin is listed below (Table 1). The chemical structure and photographic image of the resin is presented in Figure 1. Other reagents, including NaCl (Wards Science, Rochester, NY, USA), D(+) glucose, (anhydrous, 99%, Alfa Aser, Tewksbury, MA, USA), and  $\gamma$ -valerolactone (Sigma-Aldrich, St. Louis, MO, USA), were purchased at their analytical grade. All the other chemicals were used as purchased without any preliminary treatment.

**Table 1.** General information about the Amberlyst<sup>®</sup> 15 (H) ion-exchange resin.

Matrix	Type	Functional Group	Surface Area	Average Pore Diameter	Moisture Content	Physical Form	Mesh Size
Styrene divinylbenzene	Beads	Sulfonic acid	45 m <sup>2</sup> /g	24 nm	≤1.5%	Brown spherical beads	20–60 mesh

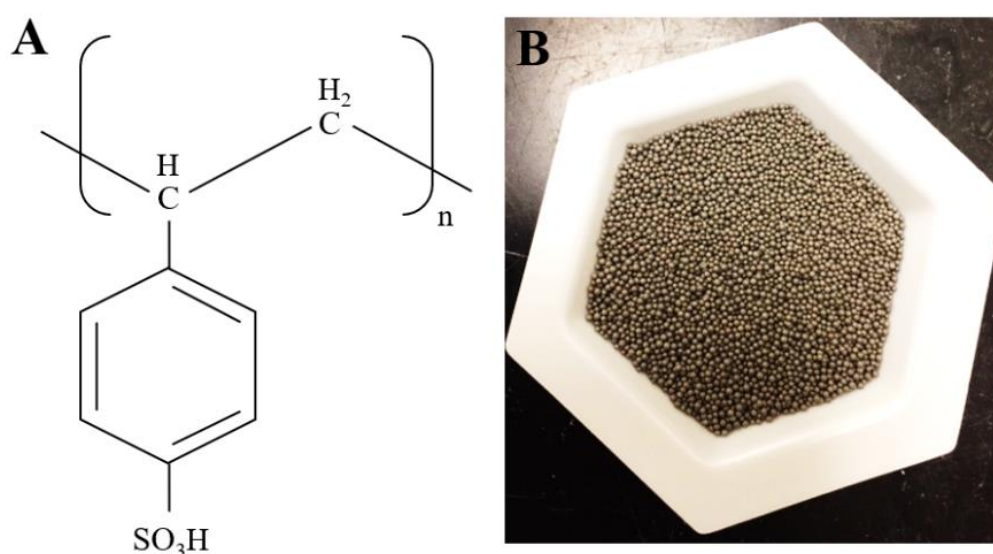


**Figure 1.** (A) Chemical structure; and (B) Photographic image of the Amberlyst<sup>®</sup>15 (H) ion-exchange resin.

## 2.2. Solution Preparation and Experimental Method

The ion-exchange resin (Amberlyst® 15 (H)) was used to remove IL from the mixture of IL, glucose, and GVL, a major component of cellulose-hydrolyzed solution. Batch adsorption experiments were performed in 5 mL glass vials containing different amounts of resin and different volumes of aqueous solution containing different concentrations of glucose, IL, and GVL. The vials were shaken at 120 rpm in a shaker (VWR Standard Analog shaker) for different times (2–150 min) under ambient condition (25 °C) to evaluate the adsorption equilibrium. After equilibrium was attained, the supernatant was taken, and the concentration of the IL was determined using a spectrophotometer (Genesys 10S UV-Vis, Thermo Scientific, Waltham, MA, USA) at the wavelength of 221 nm for the imidazolium ring. This wavelength was chosen as a working wavelength based on the maximum absorbance of the IL observed on full wavelength scanning spectra, as shown in Supplementary Information (SI) Figure S1. The impact of the operational parameters such as the amount of resin, concentration of IL, GVL, and glucose, and contact time were investigated to determine the optimum conditions. All the experimental results were measured in triplicate, the data were averaged, and an error of 8% was observed.

The total IL [Emim] adsorbed ( $q$ ) on the resin was determined using the following mass balance equation [40]:

$$m(q_e - q_0) = V(C_i - C_j) \quad (1)$$

Initially, when fresh resin was taken,  $q_0 = 0$ . Therefore, the equation can be modified as

$$q_e = \frac{V}{m}(C_i - C_j) \quad (2)$$

where  $q_e$  = amount of [Emim] adsorbed on the resin,  $V$  = volume of the solution (L),  $m$  = amount of resin taken (g), and  $C_i$  and  $C_j$  are the initial and final [Emim] concentration (mg/L), respectively.

Similarly, the percentage removal of IL from aqueous solutions at different conditions was evaluated considering the following relation [20]:

$$\% \text{ removal} = \frac{C_i - C_j}{C_i} \times 100, \quad (3)$$

where  $C_i$  and  $C_j$  are the [Emim] concentration (mg/L) in the solution before and after adsorption, respectively.

For quantitative determination of the IL adsorbed, the standard calibration curve of the IL solution with different concentrations (10–200 mg/mL) was constructed as shown in Figure S2. This standard plot was then used to determine the IL concentration based on the absorbance of the IL solution.

Generally, sorption kinetics depends on the physical and/or chemical characteristics of the sorbent materials that ultimately influence the sorption mechanism. For a given system, it is thus always essential to estimate the rate at which sorption takes place. Kinetic models based on solution concentration are used to explain the adsorption mechanisms that typically describe the reaction order of the adsorption systems. Among others, pseudo-first-order, pseudo-second-order, and intraparticle diffusion models possessing least physical background are ordinarily used models in batch adsorption experiments. Thus, in this experiment, we considered the as-mentioned three models to understand the adsorption behavior.

The equation primarily used to explain the pseudo-first-order sorption mechanism is expressed as [41]

$$\frac{dq_t}{dt} = k_1(q_e - q_t) \quad (4)$$

The use of the linearized form of the model to determine the adsorption kinetic parameters is a common practice. Thus, on integrating the expression for the boundary

conditions  $t = 0$  to  $t = t$  and  $q_t = 0$  to  $q_t = q_t$ , a linear form of the equation is obtained as [42,43]

$$\log(q_e - q_t) = \log(q_t) - \frac{k_t}{2.303} \times t, \quad (5)$$

where  $q_e$  = adsorbed IL at equilibrium, (mg/g);  $q_t$  = adsorbed IL at time  $t$ , (mg/g); and  $k_t$  = equilibrium rate constant ( $\text{min}^{-1}$ ).

The pseudo-second-order kinetics model describes the chemisorption or sorption processes involving chemical bonding between the adsorbate and functional group of adsorbents. Similarly, it is accepted that the pseudo-second-order model gives superior fitting to the other models. Using this kinetic model, kinetic data for a wide range of systems possessing various reaction mechanisms, including where diffusion control is to be expected, can also be easily fitted [44,45]. The term "pseudo" inferred that the rate law for adsorption is being formulated in terms of amount adsorbed ( $q$ ) instead of concentration ( $c$ ) of the adsorbing species. The expression used to explain the pseudo-second-order mechanism is as follows [43]:

$$\frac{dq_t}{dt} = k_2(q_e - q_t)^2 \quad (6)$$

The linearized expression obtained after integration followed by rearrangement is written as

$$\frac{t}{q_t} = \frac{1}{K_2 q_e^2} + \frac{t}{q_e}, \quad (7)$$

where  $K_2$  = equilibrium rate constant (g/mg·min).

To further investigate whether the diffusional mass transfer of the adsorbent occurs within the internal or external pores of the resin or a combination of both, the diffusional model was considered. The equation for the diffusion model (intraparticle) [46,47] is represented as

$$q_t = K_i t^{1/2} + C, \quad (8)$$

where  $q_t$  = adsorption capacity at a given time (mg/g),  $K_i$  = intraparticle diffusion rate constant ( $\text{mg/g min}^{1/2}$ ) (mg/g·min), and  $C$  = boundary thickness.

Similarly, the desorption efficiency of the adsorbed IL was determined using NaCl as a stripping agent. As required, different concentrations (0.0–4.0 M) and volumes (0–8 mL) of NaCl were added to the ion-exchange resin laden with IL. The mixture was then shaken in a shaker (120 rpm) for different time intervals (0–150 min), as required by the experimental plan. After the desorption equilibrium was attained, the IL's [Emim] concentration in the aqueous solution was estimated using a UV-Vis spectrophotometer. The amount of IL [Emim] desorbed (desorption capacity) was calculated using the relation as follows [48]:

$$q_{e2} = \frac{C_{\text{des}} \times V}{m}, \quad (9)$$

where  $q_{e2}$  = amount of [Emim] desorbed into the solution (mg/g),  $V$  = volume of the desorbing solution (L),  $m$  = amount of the resin taken (g), and  $C_{\text{des}}$  = concentration of IL [Emim] in the solution.

### 3. Results and Discussion

Considering the presence of different constituents like glucose, IL, GVL, etc., in the hydrolysate mixture, different model solutions with a single component, or mixture, were prepared, and the consequences of each component on the IL adsorption efficiency were studied.

#### 3.1. Adsorption Affinity of Resin Using Single Component (IL Only)

A prime driving force to control the mass transfer resistance of adsorbate molecules between the aqueous and solid phases is generally imparted by the initial concentration of the adsorbate [49]. To understand the influence of the IL's concentration on the adsorption

efficiency, a series of various concentrations of IL adsorption were carried out and the experimental outcomes are presented in Figure 2A. The adsorption capacity of IL increases with the initial concentration and the maximum adsorption capacity of the Amberlyst resin towards IL was found to be 245 mg/g. When the resin dosage was constant, there was a fixed amount of  $H^+$  as an exchangeable ion on the adsorbent. When the amount of IL per volume of the solution was increased, the ratio of IL to exchangeable  $H^+$  also increased. This evokes a higher driving force to subjugate the mass transfer resistance between the aqueous and solid phase, giving rise to faster adsorption. Therefore, more of the IL ions in the solution can be exchanged into the resin, resulting in an increased adsorption capacity. Moreover, as the initial concentration of IL increased from 20 mg/mL to 180 mg/mL, the adsorption percentage decreased from 94% to 54%. This is because an increase in initial IL concentration in the solution mixture will cause the adsorption site on the resin surface to become saturated, which ultimately lowers the removal percentage [50].

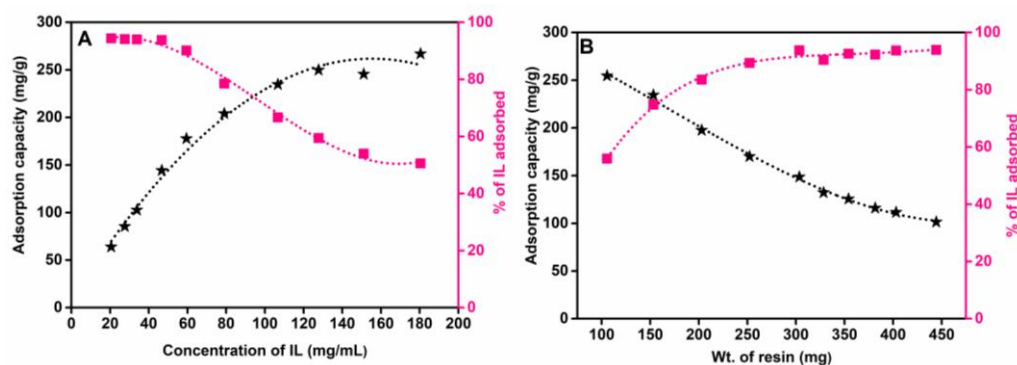


**Figure 2.** (A) Adsorption capacity of Amberlyst resin as a function of IL's initial concentration. Amount of resin taken:  $305 \pm 5$  mg, equilibration time: 1 h; (B) Different amount of resin at a given concentration of IL:  $47.7 \pm 1$  mg/mL and equilibration time: 1 h.

The adsorbent dosage has consequential influence on the adsorption capacity. This ascertains the capacity of the adsorbent for a given initial concentration of the adsorbate at the given operating conditions. The dependence of IL as a function of adsorbent dosage was evaluated by varying the amount of resin. As shown in Figure 2B, with an increase in adsorbent (resin) dosage from 100 mg to 450 mg/mL, the adsorption capacity was decreased gradually from 250 mg/g to 97 mg/g, respectively. It is presumed that as the amount of resin increased, the number of  $H^+$  ions on the resin surface increased, but the initial concentration of IL was fixed, generating the excess adsorption sites and ultimately decreasing the adsorption capacity of IL [23,51]. On the other hand, the adsorption percentage of IL increased up to an optimum dosage (300 mg/mL) of resin, beyond which the removal efficiency (94%) did not significantly change. It is predicted that, with the increase in resin dosage, the total adsorption surface site increases, leading to the increase in the absolute amount of  $H^+$  on the adsorption surface available for IL molecules. The constancy in the percentage adsorption beyond 300 mg/mL implies the saturation of the adsorption in the resin.

Another important parameter that needs to be considered during the recovery of IL from the hydrolysate mixture is the contact time of the adsorbate (IL) and adsorbent (Amberlyst resin). To investigate the adsorption equilibrium, the adsorption of IL onto Amberlyst resin was studied as a function of contact time, considering the resin amount and initial IL concentration as constant. Figure 3A illustrates the adsorption capacity of IL onto the resin as a function of time. A high initial slope for the adsorption curve was observed. Adsorption capacity increased as the equilibration time proceeded and approached to a stable value of 145 mg/g after 15 min under the experimental condition in this study. Although a 20 min contact time seems sufficient to attain the adsorption equilibrium, to ensure quantitative adsorption and effective ion pair formation between the [Emim] anion and cationic part of resin, an equilibrium time of 1 h was used in the rest of the experiments.

The rapid increase in adsorption efficiency is due to the availability of a large surface area that promotes the fast contact reaction between the IL and resin. This is presumed since, at the initial stage of the sorption process, the majority of the reaction sites are unoccupied and, hence, the extent of uptake is high. After a rapid initial adsorption, the adsorption capacity was constant due to almost complete saturation of the active sites.

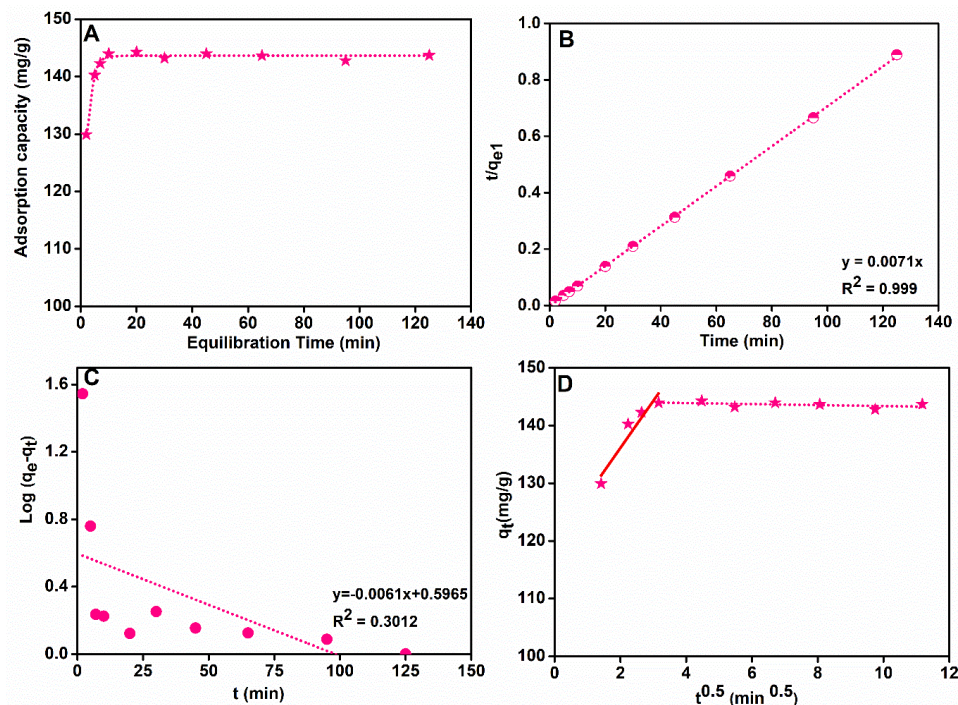


**Figure 3.** (A) Equilibrium adsorption time of IL on the Amberlyst resin; (B) Pseudo-second-order kinetic model fitting; (C) Pseudo-first-order kinetic model fitting; (D) Diffusion kinetic model fitting. Weight of resin:  $307 \pm 7$  mg, concentration of IL: 48.6 mg/mL.

The uptake rate of IL from the solution can be predicted by adsorption kinetics. Three mathematical models, namely pseudo-first-order, pseudo-second-order, and diffusion model equations, were used to fit the uptake rate using the IL adsorption data at different contact times. The adsorption kinetics studied plot in Figure 3B showed that the pseudo-second-order chemical reaction kinetic gives the best correlation of the experimental data with a higher  $R^2$  ( $=0.999$ ) value. It was thus anticipated that chemisorption is the rate-limiting step for IL adsorption in the given study. The pseudo-first-order kinetic model in Figure 3C showed  $R^2 = 0.3012$ , suggesting that the adsorption of IL on Amberlyst resin does not follow this adsorption model. Similarly, the plot of  $q_t$  versus  $t^{1/2}$ , based on the diffusion model, as shown in Figure 3D, displays a multilinear curve which does not pass through the origin. Generally, the initial stage of the curve is responsible for external mass transfer, while the next stage of the curve implies the intraparticle diffusion of IL within the pores of the resin [52]. This suggests that intraparticle diffusion is not the sole rate-limiting step. Moreover, it is anticipated that multiple adsorption processes like external diffusion as well as active sites adsorption are instantaneously involved during the adsorption of IL on the resin. It can thus be apprehended that, in the first step, the mass transfer of IL (adsorbate) from the bulk of the solution mixture to the surrounding film of adsorbents (resin) takes place. The second step is dominated by transport of the IL (adsorbate) from the film to the outer surface of the resin (adsorbent). These adsorbates can also further migrate through the pores to the inner side of the adsorbent and sequentially attached to the active sides via the ion-exchange process. In addition, the suitability of the second-order kinetic model also supports that the IL molecules can be easily adsorbed onto the adsorption sites of the resin surface through chemically dominant chemisorption interaction. The schematic of the IL adsorption through the ion-exchange process is displayed in Figure 4.

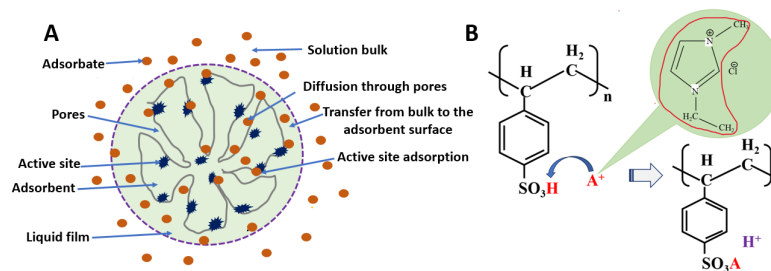


**Figure 4.** Schematic of: (A) Adsorption kinetics mass transfer processes; (B) Mechanism of ion exchange of cationic part of the IL with  $\text{H}^+$  ion on ion-exchange resin (Amberlyst 15(H)).

### 3.2. Adsorption Affinity of Resin When Multiple Components (IL+GVL+ Glucose) Are Present

There are various kinds of components in the hydrolysate mixture especially sugars, GVL, and IL. So, the effectiveness of the resin for the removal of IL from the synthetic solution mixture was also carried out by introducing different components (glucose, GVL) to the solution containing IL. Considering each kind of components as an interfering agent, solutions of IL containing different concentrations of glucose/GVL were prepared and the adsorption efficiency was studied, while keeping other variables constant. GVL, as a solvent, in the catalytic hydrolysis reaction of biomass generally increases the reaction rate compared to other solvents like water. Thus, it has been excessively used as a solvent in biomass-processing reactions [53]. Figure 5A depicts the influence of GVL on the adsorption efficiency of the Amberlyst resin towards IL. The presence of GVL in the solution mixture shows no significant interference on the adsorption capacity of IL. Moreover, a slight decrease in the adsorption percentage was observed at GVL concentrations between 170 mg/mL and 225 mg/mL. However, even at such a higher concentration of GVL, the adsorption decline exceeded 7%. Similarly, the inhibiting effect of glucose on the adsorption efficiency of IL was studied considering the different concentrations of glucose (10–50 mg/mL). The obtained result (Figure 5B) suggested that the value of the adsorption capacity and adsorption percentage of IL remains unchanged even in the presence of the multicomponent system. This adsorption behavior suggests that there is no competition between the adsorbates (IL and glucose) towards the same adsorbing site. It can thus be concluded that the Amberlyst resin could remove IL from the mixed solution effectively. Likewise, the effect of the Amberlyst resin dosage on the ion-exchange recovery of IL from the mixture of the IL, glucose, and GVL was tested in the range from 50 mg to 450 mg resin while keeping other parameters constant. The ion-exchange results (Figure S3) demonstrate that the IL recovery percentage increases from 33.5% to 76.69% when the amount of resin increases from 50 mg to 450 mg/mL from the mixture of IL ( $75 \pm 2$  mg/mL), GVL (76 mg/mL), and glucose (50 mg/mL). Such a trend is predictable due to the increased number of vacant sites on the resin surface at higher dosages when keeping the IL molecules constant.

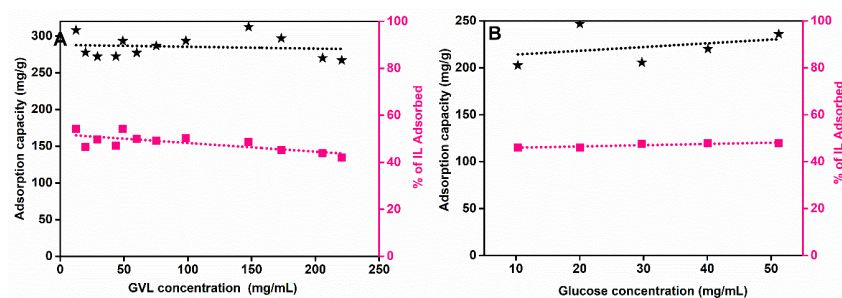


**Figure 5.** Effect of (A) GVL concentration on the adsorption capacity of Amberlyst resin towards the IL. IL concentration:  $75 \pm 1$  mg/mL, resin amount:  $303 \pm 3$  mg, adsorption time: 1 h; (B) Glucose concentration (10–50 mg/mL) on the adsorption capacity of Amberlyst resin, IL concentration:  $80 \pm 5$  mg/mL, resin amount:  $305 \pm 5$  mg, GVL:  $76 \pm 2$  mg/mL, and adsorption time: 1 h.

### 3.3. Desorption Affinity of the Adsorbed IL Using Aqueous NaCl

It is always essential to recover the adsorbed IL and reuse it. The execution of the intact back-extraction process relies on various parameters, in particular, the solvent that is used for desorption should possess sufficient capacity to promote the foremost stripping of the intended compounds. In this study, regeneration of the IL absorbed on the surface of Amberlyst resin was carried out by treating it with NaCl solution. The exhausted Amberlyst resin was mixed with NaCl followed by agitation, in which way the IL was regenerated. The effects of several desorption conditions including the concentration of stripping agent (NaCl), volume, equilibration time, etc., were investigated and discussed.

The influence of desorption time was studied for IL by varying the different stirring times from 2 to 150 min. The desorption time profile is displayed in Figure 6A. The recovery of IL increased rapidly with the increase in the extraction time from 2 to 20 min. The desorption equilibrium was attained in about 15 min and reached a maximum at 20 min. Under equilibrium conditions, the highest recovery obtained was 67%. Thereafter, no additional recovery was observed when the extraction time was increased further up to 150 min. Similarly, a series of experiments were performed by varying the NaCl concentration from 0.5 M to 4.0 M considering a volume ratio of 1:1. As shown in Figure 6B, the recovery of IL increased with increasing NaCl concentration, with a maximum of 180 mg/g from 275 mg/g of the adsorbed IL. This recovery is around 67% with respect to the adsorbed IL in 4 M NaCl solution. Furthermore, Figure 6C depicts the effect of stripping volume ratio of NaCl on the desorption of IL. The desorption of IL increases with the increase in NaCl volume ratio. At a NaCl volume ratio of 8, recoveries of IL reached almost 95%. The regeneration of the bounded IL was executed through displacement, with the like-charged species ( $\text{Na}^+$ ) in the solution having the greater electronic affinity to the resin. In this typical single-phase ion-exchange separation, the displaced IL ions were then readily removed as IL through combining with  $\text{Cl}^-$  present in the stripping solvent, as depicted by the following reactions [54].

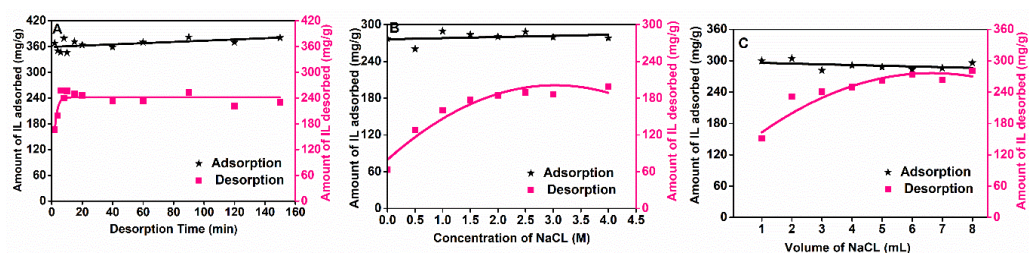


**Figure 6.** (A) Different desorption time of IL; NaCl = 4 M, IL = 75.25 mg/mL, resin =  $305 \pm 3$  mg, GVL = 75.1 mg/mL, glucose = 50 mg/mL, solvent ratio = 1:1; (B) Different concentration of NaCl (0.5–4.0 M), solvent ratio = 1:1, resin  $305 \pm 3$  mg, time = 1 h, (IL = 82.5 mg/mL, GVL = 75.1 mg/mL, and glucose = 50 mg/mL). (C) Different volume ratio of NaCl (1:1–8), (IL = 90.25 mg/mL, GVL = 75.1 mg/mL, and glucose = 50 mg/mL), resin =  $305 \pm 3$  mg, NaCl concentration = 4 M, time = 1 h.

### 3.4. Adsorption of IL from Biomass Hydrolysate Sample

The results in Figure 7 illustrate the separation efficiency of IL from the real biomass hydrolysate solution. The hydrolysate sample was obtained from the Department of Biomedical Engineering, University of Arkansas, Fayetteville. During the catalytic hydrolysis of biomass, the ratio of GVL to IL taken was 7:3. The hydrolysate being colored, as shown in Figure 7A, interferes with absorbance when the spectrophotometer was used. Considering the interference of the color component that was present in the hydrolysate, we use high-performance liquid chromatography (HPLC) for the evaluation of adsorption

efficiency of Amberlyst resin towards the IL present in the biomass hydrolysate. In this process, a HPLC system (1260 Infinity, Agilent Technology, Santa Clara, CA, USA) with a refractive index detector (RID) and a 300 mm × 7.8 mm Aminex HPX-87 H ion-exchange column (Bio-Rad, Life Science Group, Hercules, CA, USA) was used. A 5 mmol/L H<sub>2</sub>SO<sub>4</sub> solution was used as a mobile phase with the flow rate 0.5 mL/min. The injection volume was fixed to 10 µL and the column temperature was 65 °C. Prior to the adsorption experiment, solid residue was sedimented and the supernatant solution was filtered using a 0.22 µm nylon syringe filter. Different weights of resin (200–400 mg/mL) were taken in a glass vial and the desired volume of hydrolysate was mixed and shaken in a shaker for 2 h to attain the adsorption equilibrium. The desired volume of supernatant was taken and evaluated via HPLC. Figure 7B is the HPLC chromatograms of the hydrolysate before and after adsorption. A clear decrease in the IL peak intensity was observed with the different weights of resin used. Figure 7C represents the percentage of the IL adsorbed with resin mass. An increase in the adsorption percentage with increase in the amount of resin was observed reaching 51% at 400 mg/mL of resin. An increase in the percentage of adsorption of IL may be concluded due to the increase in the adsorbent surface areas and, therefore, the availability of more adsorption sites. It is also observed from HPLC spectra analysis that unwanted byproducts produced during the hydrolysis also interfere with the adsorption of IL on the resin surface.

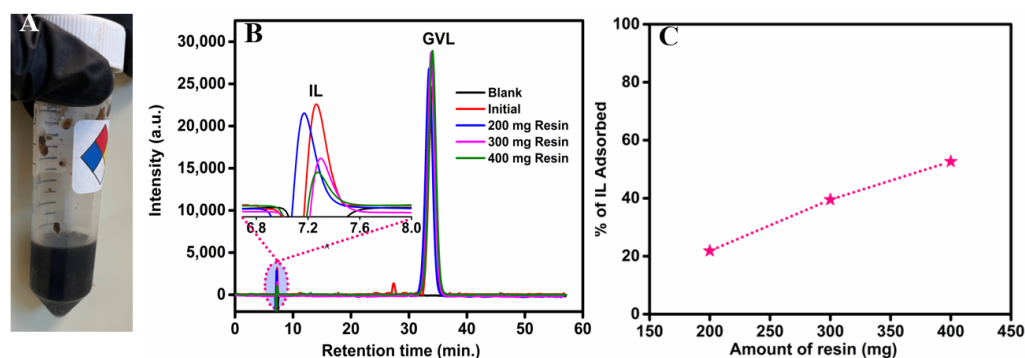


**Figure 7.** (A) Photograph of the cellulose hydrolysate product with GVL: IL is 7:3; (B) HPLC spectra showing the change in IL peak intensity before and after adsorption; (C) % of IL adsorbed at different weight of resin.

#### 4. Conclusions

In this study, we introduced an innovative approach by employing the absorption–desorption strategy to recover and recycle IL from a model cellulose hydrolysate mixture using sulphonic acid cation-exchange resin (Amberlyst 15(H)). Notably, this marks the first instance of utilizing Amberlyst 15(H) to remove IL from the hydrolysate mixture. Our findings demonstrate that over 94% of [Emim]Cl can be adsorbed by the resin within a short equilibration time of 20 min. Coexisting components such as glucose and GVL were found to have no significant impact on IL adsorption. The adsorption mechanism adhered to the pseudo-second-order process. Regeneration tests using NaCl revealed a remarkable 70% recovery of adsorbed IL. Similarly, using real hydrolysate samples, the adsorption efficiency of IL reached 51%. Notably, NaCl emerged as a superior, cost-effective, and non-corrosive stripping agent compared to HCl and NaOH for IL regeneration. This study establishes Amberlyst as a highly promising, economical ion-exchange resin for the effective separation of IL from hydrolysate solutions.

**Supplementary Materials:** The following supporting information can be downloaded at: <https://www.mdpi.com/article/10.3390/pr12010055/s1>, Figure S1: Adsorption spectra of IL; Figure S2: Calibration curve for the quantitative determination of IL adsorbed; Figure S3: IL adsorption efficiency from the mixture of IL (75 ± 2 mg/mL), GVL (76 mg/mL) and glucose (50–450 mg/mL) and equilibration time of 1 h.

**Author Contributions:** C.R.—conceptualization, methodology, formal analysis, investigation, data curation, writing—original draft preparation; C.T.—writing—review and editing, analysis, Z.Z.—hydrolysate preparation, methodology, X.Q.—supervision, conceptualization, project administration, resource management; S.R.W.—funding acquisition, supervision, writing—reviewing and editing. All authors have read and agreed to the published version of the manuscript.

**Funding:** This research was funded by the Sun Grant: AWD-101823.

**Data Availability Statement:** Data are contained within the article and supplementary materials.

**Acknowledgments:** The authors would like to acknowledge the University of Arkansas libraries for supporting the fund for open access publishing. We also would like to acknowledge Xiaolei Hao for HPLC troubleshooting and Ronny Horax for assisting with the materials and chemicals required for the experiment.

**Conflicts of Interest:** The authors declare no conflict of interest.

## References

1. Soccol, C.R.; Faraco, V.; Karp, S.; Vandenberghe, L.P.S.; Thomaz-Soccol, V.; Woiciechowski, A.; Pandey, A. Chapter 5—Lignocellulosic Bioethanol: Current Status and Future Perspectives. In *Biofuels*; Pandey, A., Larroche, C., Ricke, S.C., Dussap, C.-G., Gnansounou, E., Eds.; Academic Press: Amsterdam, The Netherlands, 2011; pp. 101–122.
2. Amini, E.; Valls, C.; Roncero, M.B. Ionic liquid-assisted bioconversion of lignocellulosic biomass for the development of value-added products. *J. Clean. Prod.* **2021**, *326*, 129275. [[CrossRef](#)]
3. Hou, Q.; Ju, M.; Li, W.; Liu, L.; Chen, Y.; Yang, Q. Pretreatment of Lignocellulosic Biomass with ionic liquids and Ionic Liquid-Based Solvent Systems. *Molecules* **2017**, *22*, 490. [[CrossRef](#)] [[PubMed](#)]
4. Silveira, M.H.L.; Morais, A.R.C.; da Costa Lopes, A.M.; Oleksyszzen, D.N.; Bogel-Lukasik, R.; Andreaus, J.; Ramos, L.P. Current Pretreatment Technologies for the Development of Cellulosic Ethanol and Biorefineries. *ChemSusChem* **2015**, *8*, 3366–3390. [[CrossRef](#)] [[PubMed](#)]
5. Morais, E.S.; Lopes, A.M.d.C.; Freire, M.G.; Freire, C.S.R.; Coutinho, J.A.P.; Silvestre, A.J.D. Use of ionic liquids and deep eutectic solvents in polysaccharides dissolution and extraction processes towards sustainable biomass valorization. *Molecules* **2020**, *25*, 3652. [[CrossRef](#)] [[PubMed](#)]
6. Bhutto, A.W.; Qureshi, K.; Harijan, K.; Abro, R.; Abbas, T.; Bazmi, A.A.; Karim, S.; Yu, G. Insight into progress in pre-treatment of lignocellulosic biomass. *Energy* **2017**, *122*, 724–745. [[CrossRef](#)]
7. New, E.K.; Tnah, S.K.; Voon, K.S.; Yong, K.J.; Procentese, A.; Shak, K.P.Y.; Subramonian, W.; Cheng, C.K.; Wu, T.Y. The application of green solvent in a biorefinery using lignocellulosic biomass as a feedstock. *J. Environ. Manag.* **2022**, *307*, 114385. [[CrossRef](#)] [[PubMed](#)]
8. Kilpeläinen, I.; Xie, H.; King, A.; Granstrom, M.; Heikkinen, S.; Argyropoulos, D.S. Dissolution of wood in Ionic Liquids. *J. Agric. Food Chem.* **2007**, *55*, 9142–9148. [[CrossRef](#)] [[PubMed](#)]
9. Putro, J.N.; Soetaredjo, F.E.; Lin, S.-Y.; Ju, Y.-H.; Ismadji, S. Pretreatment and conversion of lignocellulose biomass into valuable chemicals. *RSC Adv.* **2016**, *6*, 46834–46852. [[CrossRef](#)]
10. Vancov, T.; Alston, A.-S.; Brown, T.; McIntosh, S. Use of ionic liquids in converting lignocellulosic material to biofuels. *Renew. Energy* **2012**, *45*, 1–6. [[CrossRef](#)]
11. Cai, H.; Li, C.; Wang, A.; Xu, G.; Zhang, T. Zeolite-promoted hydrolysis of cellulose in ionic liquid, insight into the mutual behavior of zeolite, cellulose and ionic liquid. *Appl. Catal. B* **2012**, *123–124*, 333–338. [[CrossRef](#)]
12. Zhou, J.; Sui, H.; Jia, Z.; Yang, Z.; He, L.; Li, X. Recovery and purification of ionic liquids from solutions: A review. *RSC Adv.* **2018**, *8*, 32832–32864. [[CrossRef](#)] [[PubMed](#)]
13. Zhang, L.; Zhang, J.; Fu, H.; Zhang, H.; Liu, H.; Wan, Y.; Zheng, S.; Xu, Z. Microporous zeolite-templated carbon as an adsorbent for the removal of long alkyl-chained imidazolium-based ionic liquid from aqueous media. *Microporous Mesoporous Mater.* **2018**, *260*, 59–69. [[CrossRef](#)]
14. Palomar, J.; Lemus, J.; Gilarranz, M.A.; Rodriguez, J.J. Adsorption of ionic liquids from aqueous effluents by activated carbon. *Carbon* **2009**, *47*, 1846–1856. [[CrossRef](#)]
15. Ghandi, K. A Review of ionic liquids, their limits and applications. *Green Sustain. Chem.* **2014**, *04*, 44–53. [[CrossRef](#)]
16. Taokaew, S.; Kriangkrai, W. Recent progress in processing cellulose using ionic liquids as solvents. *Polysaccharides* **2022**, *3*, 671–691. [[CrossRef](#)]
17. Shuai, L.; Luterbacher, J. Organic solvent effects in biomass conversion reactions. *ChemSusChem* **2016**, *9*, 133–155. [[CrossRef](#)] [[PubMed](#)]
18. Kaur, G.; Kumar, H.; Singla, M. Diverse applications of ionic liquids: A comprehensive review. *J. Mol. Liq.* **2022**, *351*, 118556. [[CrossRef](#)]
19. Khoo, K.S.; Tan, X.; Ooi, C.W.; Chew, K.W.; Leong, W.H.; Chai, Y.H.; Ho, S.-H.; Show, P.L. How does ionic liquid play a role in sustainability of biomass processing? *J. Clean. Prod.* **2021**, *284*, 124772. [[CrossRef](#)]

20. Sui, H.; Zhou, J.; Ma, G.; Niu, Y.; Cheng, J.; He, L.; Li, X. Removal of ionic liquids from oil sands processing solution by ion-exchange resin. *Appl. Sci.* **2018**, *8*, 1611. [[CrossRef](#)]
21. Earle, M.J.; Esperança, J.M.S.S.; Gilea, M.A.; Lopes, J.N.C.; Rebelo, L.P.N.; Magee, J.W.; Seddon, K.R.; Widegren, J.A. The distillation and volatility of ionic liquids. *Nature* **2006**, *439*, 831–834. [[CrossRef](#)]
22. Mai, N.L.; Ahn, K.; Koo, Y.-M. Methods for recovery of ionic liquids—A review. *Process Biochem.* **2014**, *49*, 872–881. [[CrossRef](#)]
23. Haerens, K.; Van Deuren, S.; Matthijs, E.; der Bruggen, B. Challenges for recycling ionic liquids by using pressure driven membrane processes. *Green Chem.* **2010**, *12*, 2182–2188. [[CrossRef](#)]
24. Schäfer, T.; Rodrigues, C.M.; Afonso, C.A.M.; Crespo, J.G. Selective recovery of solutes from ionic liquids by pervaporation—A novel approach for purification and green processing. *Chem. Commun.* **2001**, *1*, 1622–1623. [[CrossRef](#)] [[PubMed](#)]
25. Sajid, M. Magnetic ionic liquids in analytical sample preparation: A literature review. *TrAC Trends Anal. Chem.* **2019**, *113*, 210–223. [[CrossRef](#)]
26. Lê, H.Q.; Pokki, J.-P.; Borrega, M.; Uusi-Kyyny, P.; Alopaeus, V.; Sixta, H. Chemical recovery of  $\gamma$ -valerolactone/water biorefinery. *Ind. Eng. Chem. Res.* **2018**, *57*, 15147–15158. [[CrossRef](#)] [[PubMed](#)]
27. Jatoi, A.S.; Baloch, H.A.; Mazari, S.A.; Mubarak, N.M.; Sabzoi, N.; Aziz, S.; Soomro, S.A.; Abro, R.; Shah, S.F. A review on extractive fermentation via ion exchange adsorption resins opportunities, challenges, and future prospects. *Biomass Convers. Biorefin.* **2023**, *13*, 3543–3554. [[CrossRef](#)]
28. He, A.; Dong, B.; Feng, X.; Yao, S. Recovery of benzothiazolium ionic liquids from the coexisting glucose by ion-exchange resins. *J. Mol. Liq.* **2017**, *227*, 178–183. [[CrossRef](#)]
29. Lemus, J.; Palomar, J.; Heras, F.; Gilarranz, M.A.; Rodriguez, J.J. Developing criteria for the recovery of ionic liquids from aqueous phase by adsorption with activated carbon. *Sep. Purif. Technol.* **2012**, *97*, 11–19. [[CrossRef](#)]
30. Matzke, M.; Thiele, K.; Müller, A.; Filser, J. Sorption and desorption of imidazolium based ionic liquids in different soil types. *Chemosphere* **2009**, *74*, 568–574. [[CrossRef](#)]
31. Czapryński, P.; Plotka, M.; Glamowski, P.; Żukowski, W.; Bajda, T. An assessment of an ion exchange resin system for the removal and recovery of Ni, Hg, and Cr from wet flue gas desulfurization wastewater—A pilot study. *RSC Adv.* **2022**, *12*, 5145–5156. [[CrossRef](#)]
32. Müller, E. Comparison between mass transfer properties of weak-anion-exchange resins with graft-functionalized polymer layers and traditional ungrafted resins. *J. Chromatogr. A* **2003**, *1006*, 229–240. [[CrossRef](#)] [[PubMed](#)]
33. Razzaq, R.; Shah, K.H.; Fahad, M.; Naeem, A.; Sherazi, T.A. Adsorption potential of macroporous Amberlyst-15 for Cd(II) removal from aqueous solutions. *Mater. Res. Express* **2020**, *7*, 25509. [[CrossRef](#)]
34. Guimarães, D.; Leão, V.A. Batch and fixed-bed assessment of sulphate removal by the weak base ion exchange resin Amberlyst A21. *J. Hazard. Mater.* **2014**, *280*, 209–215. [[CrossRef](#)] [[PubMed](#)]
35. Wołowicz, A.; Hubicki, Z. Effect of matrix and structure types of ion exchangers on palladium(II) sorption from acidic medium. *Chem. Eng. J.* **2010**, *160*, 660–670. [[CrossRef](#)]
36. Mustafa, S.; Shah, K.H.; Naeem, A.; Ahmad, T.; Waseem, M. Counter-ion effect on the kinetics of chromium (III) sorption by Amberlyst.15 in H<sup>+</sup>, Li<sup>+</sup>, Na<sup>+</sup>, Ca<sup>++</sup>, Al<sup>+++</sup> forms. *Desalination* **2010**, *264*, 108–114. [[CrossRef](#)]
37. Nandoost, A.; Bahramifar, N.; Moghadamnia, A.A.; Kazemi, S. Adsorption of malachite green (MG) as a cationic dye on Amberlyst 15, an ion-exchange resin. *J. Environ. Public Health* **2022**, *2022*, 4593835. [[CrossRef](#)] [[PubMed](#)]
38. Vignoli, C.N.; Bahé, J.M.C.F.; Marques, M.R.C. Evaluation of ion exchange resins for removal and recuperation of ammonium–nitrogen generated by the evaporation of landfill leachate. *Polym. Bull.* **2015**, *72*, 3119–3134. [[CrossRef](#)]
39. Cren, É.C.; Meirelles, A.J.A. Adsorption isotherms for oleic acid removal from ethanol + water solutions using the strong anion-exchange resin Amberlyst A26 OH. *J. Chem. Eng. Data* **2005**, *50*, 1529–1534. [[CrossRef](#)]
40. Choi, S.B.; Won, S.W.; Yun, Y.-S. Use of ion-exchange resins for the adsorption of the cationic part of ionic liquid, 1-ethyl-3-methylimidazolium. *Chem. Eng. J.* **2013**, *214*, 78–82. [[CrossRef](#)]
41. Kyzas, G.Z.; Kostoglou, M. Green Adsorbents for Wastewaters: A Critical Review. *Materials* **2014**, *7*, 333–364. [[CrossRef](#)]
42. Hou, Y.; Liu, L.; He, Q.; Zhang, D.; Jin, J.; Jiang, B.; Zhao, L. Adsorption behaviors and kinetics studies of chitoooligosaccharides with specific degree of polymerization on a novel ion-exchange resin. *Chem. Eng. J.* **2022**, *430*, 132630. [[CrossRef](#)]
43. Sahoo, T.R.; Prelot, B. Chapter 7—Adsorption processes for the removal of contaminants from wastewater: The perspective role of nanomaterials and nanotechnology. In *Nanomaterials for the Detection and Removal of Wastewater Pollutants*; Bonelli, B., Freyria, F.S., Rossetti, I., Sethi, R., Eds.; Elsevier: Amsterdam, The Netherlands, 2020; pp. 161–222.
44. Kostoglou, M.; Karapantsios, T.D. Why is the linearized form of pseudo-second-order adsorption kinetic model so successful in fitting batch adsorption experimental data? *Colloids Interfaces* **2022**, *6*, 55. [[CrossRef](#)]
45. Xiao, Y.; Azaiez, J.; Hill, J.M. Erroneous application of pseudo-second-order adsorption kinetics model: Ignored assumptions and spurious correlations. *Ind. Eng. Chem. Res.* **2018**, *57*, 2705–2709. [[CrossRef](#)]
46. Largitte, L.; Pasquier, R. A review of the kinetics adsorption models and their application to the adsorption of lead by an activated carbon. *Chem. Eng. Res. Des.* **2016**, *109*, 495–504. [[CrossRef](#)]
47. Li, Z.; Meng, X.; Zhang, Z. Equilibrium and kinetic modelling of adsorption of Rhodamine B on MoS<sub>2</sub>. *Mater. Res. Bull.* **2019**, *111*, 238–244. [[CrossRef](#)]

48. Dada, A.O.; Adekola, F.A.; Odebunmi, E.O.; Ogunlaja, A.S.; Bello, O.S. Two–three parameters isotherm modeling, kinetics with statistical validity, desorption and thermodynamic studies of adsorption of Cu(II) ions onto zerovalent iron nanoparticles. *Sci. Rep.* **2021**, *11*, 16454. [[CrossRef](#)] [[PubMed](#)]
49. Bayramoglu, G.; Altintas, B.; Arica, M.Y. Adsorption kinetics and thermodynamic parameters of cationic dyes from aqueous solutions by using a new strong cation-exchange resin. *Chem. Eng. J.* **2009**, *152*, 339–346. [[CrossRef](#)]
50. Al-Ghouti, M.A.; Al-Absi, R.S. Mechanistic understanding of the adsorption and thermodynamic aspects of cationic methylene blue dye onto cellulosic olive stones biomass from wastewater. *Sci. Rep.* **2020**, *10*, 15928. [[CrossRef](#)]
51. Xu, M.; Ao, Y.; Wang, S.; Peng, J.; Li, J.; Zhai, M. Efficient adsorption of 1-alkyl-3-methylimidazolium chloride ionic liquids onto modified cellulose microspheres. *Carbohydr. Polym.* **2015**, *128*, 171–178. [[CrossRef](#)]
52. Olu-Owolabi, B.I.; Diagboya, P.N.; Adebowale, K.O. Evaluation of pyrene sorption–desorption on tropical soils. *J. Environ. Manag.* **2014**, *137*, 1–9. [[CrossRef](#)]
53. Mellmer, M.A.; Alonso, D.M.; Luterbacher, J.S.; Gallo, J.M.R.; Dumesic, J.A. Effects of  $\gamma$ -valerolactone in hydrolysis of lignocellulosic biomass to monosaccharides. *Green Chem.* **2014**, *16*, 4659–4662. [[CrossRef](#)]
54. Corley, C.A.; Iacono, S.T. Recycling of 1,2-dimethyl-3-propylimidazolium bis(trifluoromethylsulfonyl)imide ionic liquid by stacked cation and anion exchange adsorption-desorption. *Separations* **2019**, *6*, 29. [[CrossRef](#)]

**Disclaimer/Publisher’s Note:** The statements, opinions and data contained in all publications are solely those of the individual author(s) and contributor(s) and not of MDPI and/or the editor(s). MDPI and/or the editor(s) disclaim responsibility for any injury to people or property resulting from any ideas, methods, instructions or products referred to in the content.